



**HAL**  
open science

## **Sinking *Trichodesmium* fixes nitrogen in the dark ocean**

Mar Benavides, Sophie Bonnet, Frédéric a C Le Moigne, Gabrielle Armin,  
Keisuke Inomura, Søren Hallstrøm, Lasse Riemann, Ilana Berman-Frank,  
Emilie Poletti, Marc Garel, et al.

► **To cite this version:**

Mar Benavides, Sophie Bonnet, Frédéric a C Le Moigne, Gabrielle Armin, Keisuke Inomura, et al..  
Sinking *Trichodesmium* fixes nitrogen in the dark ocean. *The International Society of Microbiological  
Ecology Journal*, 2022, 16 (10), pp.2398-2405. 10.1038/s41396-022-01289-6 . hal-03986959

**HAL Id: hal-03986959**

**<https://hal.science/hal-03986959v1>**

Submitted on 13 Feb 2023

**HAL** is a multi-disciplinary open access archive for the deposit and dissemination of scientific research documents, whether they are published or not. The documents may come from teaching and research institutions in France or abroad, or from public or private research centers.

L'archive ouverte pluridisciplinaire **HAL**, est destinée au dépôt et à la diffusion de documents scientifiques de niveau recherche, publiés ou non, émanant des établissements d'enseignement et de recherche français ou étrangers, des laboratoires publics ou privés.

1 **Sinking *Trichodesmium* fixes nitrogen in the dark ocean**

2

3 Mar Benavides<sup>1,2,\*</sup>, Sophie Bonnet<sup>1</sup>, Frédéric A. C. Le Moigne<sup>1,3</sup>, Gabrielle Armin<sup>4</sup>,  
4 Keisuke Inomura<sup>4</sup>, Søren Hallstrøm<sup>5</sup>, Lasse Riemann<sup>5</sup>, Ilana Berman-Frank<sup>6</sup>, Emilie  
5 Poletti<sup>1</sup>, Marc Garel<sup>1</sup>, Olivier Grosso<sup>1</sup>, Karine Leblanc<sup>1</sup>, Catherine Guigue<sup>1</sup>, Marc  
6 Tedetti<sup>1</sup>, Cécile Dupouy<sup>1</sup>

7

8 <sup>1</sup>Aix Marseille Univ, Université de Toulon, CNRS, IRD, MIO UM 110, 13288, Marseille,  
9 France

10 <sup>2</sup>Turing Center for Living Systems, Aix-Marseille University, 13009 Marseille, France

11 <sup>3</sup>LEMAR, Laboratoire des Sciences de l'Environnement Marin, UMR6539, CNRS, UBO,  
12 IFREMER, IRD, 29280 Plouzané, Technopôle Brest-Iroise, France

13 <sup>5</sup>Graduate School of Oceanography, University of Rhode Island, South Kingstown, RI,  
14 USA

15 <sup>5</sup>Marine Biological Section, Department of Biology, University of Copenhagen, Helsingør,  
16 Denmark

17 <sup>6</sup>Department of Marine Biology, Leon H. Charney School of Marine Sciences, University  
18 of Haifa, Mt. Carmel, Haifa, Israel

19

20 \*Mar Benavides [mar.benavides@ird.fr](mailto:mar.benavides@ird.fr)

21

22 **Competing Interests Statement:** Authors declare that they have no competing  
23 interests.

24 **Abstract**

25

26 The photosynthetic cyanobacterium *Trichodesmium* is widely distributed in the surface  
27 low latitude ocean where it contributes significantly to N<sub>2</sub> fixation and primary  
28 productivity. Previous studies found *nifH* genes and intact *Trichodesmium* colonies in the  
29 sunlight-deprived meso- and bathypelagic layers of the ocean (200-4 000 m depth). Yet,  
30 the ability of *Trichodesmium* to fix N<sub>2</sub> in the dark ocean has not been explored. We  
31 performed <sup>15</sup>N<sub>2</sub> incubations in sediment traps at 170, 270 and 1 000 m at two locations in  
32 the South Pacific. Sinking *Trichodesmium* colonies fixed N<sub>2</sub> at similar rates than  
33 previously observed in the surface ocean (36-214 fmol N cell<sup>-1</sup> d<sup>-1</sup>). This activity  
34 accounted for 40 ± 28 % of the bulk N<sub>2</sub> fixation rates measured in the traps, indicating  
35 that other diazotrophs were also active in the mesopelagic zone. Accordingly, cDNA *nifH*  
36 amplicon sequencing revealed that while *Trichodesmium* accounted for most of the  
37 expressed *nifH* genes in the traps, other diazotrophs such as *Chlorobium* and  
38 Deltaproteobacteria were also active. Laboratory experiments simulating mesopelagic  
39 conditions confirmed that increasing hydrostatic pressure and decreasing temperature  
40 reduced but did not completely inhibit N<sub>2</sub> fixation in *Trichodesmium*. Finally, using a cell  
41 metabolism model we predict that *Trichodesmium* uses photosynthesis-derived stored  
42 carbon to sustain N<sub>2</sub> fixation while sinking into the mesopelagic. We conclude that  
43 sinking *Trichodesmium* provides ammonium, dissolved organic matter and biomass to  
44 mesopelagic prokaryotes.

45 **Introduction**

46

47 Dinitrogen (N<sub>2</sub>) fixing prokaryotes (diazotrophs) supply bioavailable nitrogen to  
48 planktonic communities, fueling primary production and contributing to carbon export in  
49 the ocean [1]. Nitrogen inputs by diazotrophs may become even more important in the  
50 future ocean, as global warming enhances water column stratification constraining  
51 nitrogen availability for primary producers [2]. Early studies suggested that diazotrophs  
52 were only present in low latitude warm oligotrophic waters of the (sub)tropical ocean.  
53 However, over the past decade it has become clear that diazotrophs are also found in  
54 cold and nutrient-rich environments such as estuaries, shelf seas, polar regions and the  
55 ocean's dark pelagic realm [3]. Devoid of light, N<sub>2</sub> fixation in the dark ocean has been  
56 attributed to heterotrophic non-cyanobacterial diazotrophs presumably relying on  
57 reduced organic compounds for energy and carbon supply [4–6]. However,  
58 cyanobacterial diazotrophs have been repeatedly observed in mesopelagic to  
59 bathypelagic depths (200 to 4 000 m; Table S1; [7]).

60

61 The filamentous cyanobacterium *Trichodesmium* thrives in tropical and subtropical  
62 ocean's photic zone where it can introduce 60-80 Tg N y<sup>-1</sup>, representing roughly half of  
63 the reactive nitrogen input to the global ocean [8]. *Trichodesmium* has gas vesicles  
64 which confer cells with buoyancy, restricting their vertical distribution in the water column  
65 [9, 10]. Accordingly, *Trichodesmium* biomass is thought to be fully remineralized within  
66 the photic zone [11]. Recently, however, molecular and imaging studies have  
67 documented intact *Trichodesmium* cells and expression of nitrogenase genes down to 4  
68 000 m depth across the world's oceans (Table S1). The mechanisms through which  
69 *Trichodesmium* sinks into the dark ocean may include gravitational sinking, downwelling

70 events [12], mineral ballasting [13], or sudden autocatalytic cell death in response to  
71 nutrient limitation [14]. Sinking velocities can be fast enough for surface photoautotrophic  
72 cells to reach the dark ocean while remaining viable [15–18], but whether sinking  
73 *Trichodesmium* remains metabolically active and carries out N<sub>2</sub> fixation in the dark ocean  
74 is not known.

75

76 If diazotrophically active *Trichodesmium* fixes N<sub>2</sub> in the dark ocean it would not only  
77 affect the global marine nitrogen inventory but conceivably also stimulate microbial  
78 processing of particulate organic matter in the (sub)tropical regions where it thrives,  
79 affecting vertical carbon export and remineralization in the dark ocean [19]. In the  
80 present study we combine <sup>15</sup>N<sub>2</sub> incubation on sediment traps, sinking simulation  
81 laboratory experiments and cell metabolism modeling to document that *Trichodesmium*  
82 can fix N<sub>2</sub> while sinking far below the photic zone, constituting a hitherto unaccounted  
83 reactive nitrogen and organic matter source in the dark ocean.

84

## 85 **Materials and Methods**

86

### 87 *Sinking particle sampling in the South Pacific Ocean*

88

89 Sinking particles were collected in the western tropical South Pacific during the TONGA  
90 cruise (doi: [10.17600/18000884](https://doi.org/10.17600/18000884)) onboard the R/V *L'Atalante* from November 1st to  
91 December 5th 2019. Surface tethered mooring lines (~1 000 m long) were deployed at  
92 two stations: S05M (21.157°S, 175.153°W, 5 days) and S10M (19.423°S, 175.133°W, 4  
93 days). The mooring lines featured three sediment traps placed at 170, 270 and 1 000 m.  
94 These depth levels were chosen to match the base of the photic layer, the usual depth to

95 calculate flux attenuation (100 m deeper than the photic layer) and the base of the  
96 mesopelagic layer, respectively. Each trap consisting of four particle interceptor tubes  
97 mounted on an articulated cross-frame. Out of the four tubes deployed per depth, two  
98 were used for this study. The first tube was filled with 6 l of 0.2  $\mu\text{m}$  filtered seawater  
99 followed by 2.5 l of a 50 g l<sup>-1</sup> saline brine labeled with <sup>15</sup>N<sub>2</sub> gas. The brine was prepared  
100 in a 4.5 l polycarbonate bottle fitted with a septum screwcap and labeled with high-purity  
101 <sup>15</sup>N<sub>2</sub> gas (Euroiso-top) injected through the septum and the bubble thoroughly mixed with  
102 the brine for several hours using a magnetic stirring plate. The brine had an enrichment  
103 ~55 <sup>15</sup>N atom % as determined by membrane inlet mass spectrometry [20]. The second  
104 tube was filled with 6 l RNAlater solution [21] and 2.5 l of non-labeled brine.

105

106 Immediately upon recovery of the traps onboard, the upper layer of the tubes was  
107 carefully removed with a peristaltic pump until the density gradient of the brine was  
108 reached. The seawater layer overlying the brine prevented potential intrusions of surface  
109 seawater when recovering the trap line onboard. We confirmed that no surface  
110 contamination occurred since the particulate organic carbon fluxes measured in brine-  
111 filled traps agreed with those measured in parallel traps kept closed during recovery  
112 onboard ('RESPIRE' traps [22]; M. Bressac, personal communication). The brine of the  
113 <sup>15</sup>N<sub>2</sub>-labeled traps was transferred to magnetic stirrer plates to ensure homogeneous  
114 aliquot sampling. Three aliquots of 50 ml were filtered onto precombusted 25 mm GF/F  
115 filters (GE Healthcare, Little Chalfont, UK) for bulk elemental analysis coupled isotope  
116 ratio mass spectrometry (EA-IRMS), and another three were filtered onto 1  $\mu\text{m}$   
117 polycarbonate filters (Nucleopore, Whatman, Maidstone, UK) and fixed with 2%  
118 microscopy grade paraformaldehyde for single-cell nanoscale secondary ion mass  
119 spectrometry (nanoSIMS) analyses (see below). Samples integrating biomass between

120 2 000 and 200 m (bottlenet [16]) were used to measure natural  $^{15}\text{N}$  atom % enrichment  
121 of bulk biomass and *Trichodesmium* cells. In parallel, the whole brine volume of the tube  
122 filled with RNAlater was immediately filtered onto 0.2  $\mu\text{m}$  polysulfone filters (Supor, Pall  
123 Gelman, Port Washington, NY, USA). The filters were transferred to bead beater tubes  
124 containing a mix of 0.1 mm and 0.5 mm silica beads, flash-frozen in liquid nitrogen and  
125 stored at  $-80^\circ\text{C}$  until RNA extractions (see below).

126

### 127 *Bulk and Trichodesmium-specific $\text{N}_2$ fixation rates*

128

129 The  $^{15}\text{N}/^{14}\text{N}$  ratio of dissolved nitrogen was measured by membrane inlet mass  
130 spectrometry and the bulk  $^{15}\text{N}/^{14}\text{N}$  ratio and particulate nitrogen concentration of particles  
131 with an Integra CN EA-IRMS (SerCon Ltd, Chesire, UK) as described elsewhere [23].  
132 The  $^{15}\text{N}$  atom % enrichment of *Trichodesmium* filaments was analyzed on a nanoSIMS  
133 50L (CAMECA, Gennevilliers, France) at the Leibniz Institute for Baltic Sea Research  
134 (IOW, Germany). Sample filters were mounted with conductive tape on 10 x 5 mm  
135 aluminum stubs (Ted Pella Inc., Redding, CA) and gold-coated to a thickness of ca. 30  
136 nm (Cressington auto sputter coater). A 1 pA 16 keV Cesium ( $\text{Cs}^+$ ) primary beam was  
137 scanned on a 512 x 512 pixel raster with a raster area of 15 x 15  $\mu\text{m}$ , and a counting  
138 time of 250  $\mu\text{s}$  per pixel. Samples were pre-sputtered with 600 pA  $\text{Cs}^+$  current for 2 min  
139 in a raster of 30 x 30  $\mu\text{m}$  to remove the gold and surface contaminants and reach the  
140 steady state of ion formation. Negative secondary ions  $^{12}\text{C}^-$ ,  $^{13}\text{C}^-$ ,  $^{12}\text{C}^{14}\text{N}^-$ ,  $^{12}\text{C}^{15}\text{N}^-$  and  $^{31}\text{P}^-$   
141 were detected with electron multiplier detectors, and secondary electrons were  
142 simultaneously imaged. Sixty serial quantitative secondary ion mass planes were  
143 generated, drift corrected and accumulated to the final image. Mass resolving power was  
144 >8 000 to resolve isobaric interferences. Data was processed using the

145 Look@nanoSIMS software [24]. Isotope ratio images were generated by dividing the  $^{13}\text{C}^-$   
146 ion count by the  $^{12}\text{C}^-$  ion count, and the  $^{12}\text{C}^{15}\text{N}^-$  ion count by the  $^{12}\text{C}^{14}\text{N}^-$  ion count pixel by  
147 pixel. Individual *Trichodesmium* filaments (trichomes) were identified in nanoSIMS  
148 secondary electron  $^{12}\text{C}^-$ ,  $^{12}\text{C}^{14}\text{N}^-$  images. These images were used to define regions of  
149 interest (ROIs). For each ROI, the  $^{13}\text{C}/^{12}\text{C}$  and  $^{15}\text{N}/^{14}\text{N}$  ratios were calculated based on  
150 the ion counts averaged over the ROIs.

151

152 Bulk  $\text{N}_2$  fixation rates were calculated following the equations of Montoya et al. [25].

153 *Trichodesmium*-specific volumetric  $\text{N}_2$  fixation rates were calculated using the following  
154 equation:

155

$$156 \quad \text{Volumetric } \text{N}_2 \text{ fixation rate} = \frac{(A_{Tricho} - A_{TrichoNat})}{(A_{N_2} - A_{TrichoNat})} \times \frac{PN_{Tricho}}{t}$$

157

158 where  $A_{Tricho}$  is the  $^{15}\text{N}$  atom% enrichment of individual *Trichodesmium* cells incubated  
159 with  $^{15}\text{N}_2$ ,  $A_{TrichoNat}$  is the natural  $^{15}\text{N}$  atom% enrichment of *Trichodesmium* as analyzed  
160 by nanoSIMS (see above),  $A_{N_2}$  is the  $^{15}\text{N}$  atom% enrichment of dissolved  $\text{N}_2$  measured  
161 by membrane inlet mass spectrometry (see above),  $PN_{Tricho}$  is the nitrogen biomass of  
162 *Trichodesmium* and  $t$  is the incubation time.  $PN_{Tricho}$  is calculated by converting  
163 *Trichodesmium nifH* gene copies  $\text{l}^{-1}$  (as provided by Bonnet et al. [26]) to carbon  
164 considering the average of the mmol C : *nifH* ratio provided in Meiler et al. [27]. Carbon  
165 is converted to nitrogen considering a C:N ratio of 6:1 [28]. *Trichodesmium* abundance is  
166 calculated by converting *Trichodesmium nifH* gene copies  $\text{l}^{-1}$  into cells  $\text{l}^{-1}$  considering a  
167 ratio of 12 and 103 *nifH* gene copies per *Trichodesmium* cell, obtained empirically for  
168 stations S05M and S10M, respectively, by comparing quantitative PCR and microscopy  
169 *Trichodesmium* counts [26]. Finally, *Trichodesmium* cell-specific  $\text{N}_2$  fixation rates (fmol N

170 cell<sup>-1</sup> d<sup>-1</sup>) are calculated by dividing volumetric rates by *Trichodesmium* abundance (cells  
171 l<sup>-1</sup>).

172

173 *RNA extractions, nifH gene sequencing and bioinformatics*

174

175 RNA was extracted using the RNeasy mini kit (Qiagen) including a 1 h on-column  
176 DNase digestion. PCRs on extracted RNA controlled for complete DNA digestion.  
177 Reverse transcription (RT) were performed with TaqMan Reverse Transcription (Applied  
178 Biosystems) using reverse primer nifH3 (5'-ATR TTR TTN GCN GCR TA-3') and 5 µl of  
179 RNA extract. Triplicate nested PCR reactions were conducted using degenerate *nifH*  
180 primers nifH1 (5'-TGYGAYCCNAARGCNGA-3'write here), nifH2 (5'-  
181 ADNGCCATCATYTCNCC-3'), *nifH3* and *nifH4* (5'-TTYTAYGGNAARGGNGG-3') [29].  
182 The PCR mix was composed of 5 µl of 5X MyTaq red PCR buffer (Bioline), 1.25 µl of 25  
183 mM MgCl<sub>2</sub>, 0.5 µl of 20 µM forward and reverse primers, 0.25 µl Platinum Taq and 5 µl  
184 of cDNA (1 µl from the first PCR reaction was used as template in the second reaction).  
185 The reaction volume was adjusted to 25 µl with PCR grade water. Triplicate PCR  
186 products were pooled and purified using the GeneClean Turbo kit (MP Biomedicals).  
187 Samples were sequenced using the Illumina MiSeq platform with 2 × 300 bp paired-end  
188 reads. Demultiplexed paired-end sequences were dereplicated, denoised, assembled  
189 and chimeras discarded using the DADA2 pipeline [30]. This generated 6 929 ASVs  
190 (146 000 ± 18 000 reads per sample). Sequences have been deposited in the Sequence  
191 Read Archive under accession number PRJNA742179. The ASVs were translated to  
192 amino acid sequences using FrameBot [31] and filtering for homologous genes was  
193 done following the NifMAP pipeline [32]. This reduced the number of ASVs to 6 503  
194 accounting for 842 515 reads (96% of all reads). Taxonomic ranks were assigned

195 according to the *nifH* gene reference database collated and maintained by the Zehr  
196 research group (v. June 2017; <https://www.jzehrlab.com/nifh>).

197

198 *Hydrostatic pressure experiments with Trichodesmium cultures*

199

200 The effect of increasing hydrostatic pressure and decreasing temperature on  
201 *Trichodesmium* was tested using a sinking particle simulator [33]. Exponentially growing  
202 cultures of *Trichodesmium erythraeum* IMS101 grown at 27°C under a 12h:12 light:dark  
203 cycle on YBCII medium [34] were transferred to four autoclaved 500 ml high pressure  
204 titanium bottles (HPBs) placed inside incubators (Mettmert IPP 750+, Schwabach,  
205 Germany) programmed to decrease temperature at the desired pace. For 360 h, the  
206 pressure within the HPBs was increased from 0 to 3 MPa using a piloted pressure  
207 generator based on a motorized syringe controlled by a computer. Pressure was logged  
208 continuously by means of a Metrolog (Metro-Mesures, Mennecy, France) and controlled  
209 by the software with a precision of 0.2%. Concomitantly, temperature of the HPBs was  
210 decreased from 27 to 14°C. These conditions simulate those experienced by cells when  
211 sinking from the surface to ~300 m depth with a conservative sinking speed of 20 m d<sup>-1</sup>  
212 (at the lower end of empirically measured *Trichodesmium* sinking velocities; Table S2).  
213 Triplicate analytical culture aliquots were sampled from two HPBs at 192 and from  
214 another two HPBs at 360 h, corresponding to simulated depths of 160 and 300 m,  
215 respectively. N<sub>2</sub> fixation incubations at these time points were done under the  
216 corresponding hydrostatic pressure conditions by 100 ml culture aliquots to pressurized  
217 titanium flasks containing 30% volume of culture medium previously enriched with <sup>15</sup>N<sub>2</sub>  
218 gas (prepared as explained above) and incubated for 24 h. Particulate and dissolved  
219 samples were analyzed by EA-IRMS and MIMS as described above. Cultures under a

220 12h:12h dark:dark cycle and temperature decrease pace identical to that of pressurized  
221 cultures were used as a control.

222

223 *Sinking Trichodesmium cell metabolism model*

224

225 We hypothesized that *Trichodesmium* fixes N<sub>2</sub> while sinking into the dark ocean at the  
226 expense of carbon accumulated from photosynthesis before starting to sink. Sinking  
227 *Trichodesmium* can thus only fix N<sub>2</sub> until reaching the depth where its carbon storage is  
228 depleted. To compute how much carbon storage *Trichodesmium* needs to acquire  
229 before sinking to be able to fix N<sub>2</sub> at 1 000 m depth, we adapted a previously published  
230 coarse-grained cell metabolism model [35]. The model simulates photosynthesis, N<sub>2</sub>  
231 fixation, and respiration for the entire trichome, resolving diffusion boundary layers for  
232 oxygen transport and distinguishing between photosynthetic and non-photosynthetic  
233 cells (Fig. S1). Photosynthetic cells fix carbon with harvested light energy, accumulate  
234 carbon, and synthesize new biomass, whereas non-photosynthetic cells use carbon  
235 stored by other cells to fix N<sub>2</sub> (Fig. S1).

236

237 To adapt the model to *Trichodesmium* colonies sinking into the mesopelagic layer we  
238 considered the variability in temperature and oxygen observed from the ocean surface to  
239 1 000 m in our study (Fig. S2) as well as the inhibiting effect of increasing nitrate  
240 concentrations on N<sub>2</sub> fixation. Walden's rule [47] was used to simulate the variation of  
241 oxygen diffusivity, as in previous studies [37], and the Arrhenius equation was used to  
242 simulate the temperature dependencies of metabolisms [35]. The adapted model was  
243 applied to *Trichodesmium* sinking from the bottom of the mixed layer (~40 m; Fig. S2)  
244 over a wide range of calculated velocities (ranging from 12 to ~600 m d<sup>-1</sup>;

245 Supplementary Methods) considering a ratio of initial carbon storage level relative to  
246 non-storage biomass ( $R_{Sto}$ ) ranging between 0 and 2. This value of  $R_{Sto}$  range is  
247 conservative, since it varies between 1 and 10 according to carbohydrate and lipid to  
248 protein ratios in various phytoplankton species [38]. To test the effect of nitrate inhibition  
249 on *Trichodesmium*'s  $N_2$  fixation in the mesopelagic, we considered a decrease in the  
250 diazotrophically active cells by 70 and 50% in each trichome. All model equations are  
251 detailed in Inomura et al. [35] and the adapted code is fully available in Zenodo  
252 (<https://zenodo.org/record/5153594>; doi: 10.5281/zenodo.5153594).

253

#### 254 Statistical analyses

255

256  $^{15}N$  atom % enrichment values were checked for normality using a Shapiro-Wilk test and  
257 significant differences between samples tested with Wilcoxon test, using R software  
258 package dplyr in RStudio Version 1.2.5033.

259

## 260 **Results and Discussion**

261

### 262 *Trichodesmium* fixes $N_2$ and expresses *nifH* in the mesopelagic ocean

263

264 The isotopic enrichment of single *Trichodesmium* filaments in the traps ranged between  
265  $0.428 \pm 0.002$  and  $0.463 \pm 0.033$   $^{15}N$  atom % (Fig. 1). The  $^{15}N$  atom % enrichment of all  
266 *Trichodesmium* filaments analyzed was significantly higher than that of filaments not  
267 incubated with  $^{15}N_2$  collected over the same depth range ( $0.364 \pm 0.006$   $^{15}N$  atom %;  
268 Wilcoxon test  $p = 0.004$  and  $p = 0.014$  for S05M and S10M, respectively; Fig. 1). The  
269 derived cell-specific  $N_2$  fixation rates ranged between 36 and 214  $fmol\ N\ cell^{-1}\ d^{-1}$  (Table

270 S3), in the same range of previous *Trichodesmium* cell-specific N<sub>2</sub> fixation  
271 measurements in surface waters of the South Pacific [39, 40]. While the salinity in the  
272 traps (~50 ppt) was higher than that of ambient waters (~34 ppt), previous studies have  
273 shown that increased salinity reduces but does not impair *Trichodesmium* growth up to  
274 42 ppt [41]. Comparing in *Trichodesmium* cultures grown on 34 and 50 ppt showed a  
275 decrease in N<sub>2</sub> fixation rates by 63 ± 15 % (Supplementary Methods). Hence, the high  
276 salinity of the <sup>15</sup>N<sub>2</sub>-labeled brine may have reduced but did not completely inhibit N<sub>2</sub>  
277 fixation in *Trichodesmium*, implying that in situ rates could be higher than measured in  
278 our traps. Overall, these cell-specific rates indicate that *Trichodesmium* sinking into the  
279 mesopelagic zone can fix N<sub>2</sub> at rates comparable to the surface.

280

281 Amplicon sequencing revealed that *nifH* gene transcripts annotated as *Trichodesmium*  
282 were present in all sediment trap samples, accounting for 26-84% (average 56%) of the  
283 sequence reads (Fig. 2). This indicates that *Trichodesmium* constituted a substantial  
284 fraction of the diazotroph community that actively transcribed the *nifH* gene in all  
285 samples (Fig. 2). However, comparing the <sup>15</sup>N<sub>2</sub> atom % enrichment of bulk sediment trap  
286 material and individual filaments, *Trichodesmium* accounted for 1 to 70% of the N<sub>2</sub>  
287 fixation activity measured in the traps (Table S3). Hence, other organisms contributed to  
288 N<sub>2</sub> fixation within the traps, which could be driven by either surface diazotrophs attached  
289 to particles or by true mesopelagic N<sub>2</sub> fixation driven by diazotrophs residing in deep  
290 waters. The contribution of *Trichodesmium* to mesopelagic N<sub>2</sub> fixation in the subtropical  
291 region studied here is notorious but likely restricted to the (sub)tropical regions where  
292 this cyanobacterium abounds. The predicted warming and expansion of oligotrophic  
293 subtropical gyres towards higher latitudes may expand the effect of sinking  
294 *Trichodesmium* to higher latitudes in the future [42].

295

296 *Crocospaera*, the only other cyanobacterial group present in the cDNA sequence data,  
297 comprised 10% of the cDNA sequence reads of station S05M at 270 m, but less than  
298 0.1% in the other samples. Sequences annotated as the genus *Chlorobium*  
299 (Bacteroidota) comprised 60% of cDNA sequences recovered from 1 000 m depth at  
300 station S05M and constituted a substantial fraction of the expression profiles of station  
301 S10M at 170 m and 270 m, comprising 16% and 20% of cDNA sequences, respectively,  
302 but their contribution was less than 1% in the rest of the samples. This indicates that,  
303 when specific conditions are met, *Chlorobium* can contribute substantially to the *nifH*  
304 transcript pool. A noteworthy contribution to the expression profiles was  
305 Alphaproteobacteria classified as the genus *Yangia* (Rhodobacteraceae [43]), which  
306 comprised approximately 10% of cDNA sequences of S05M but were virtually  
307 undetected at S10M. Both Bacteroidota and Rhodobacteraceae have been identified as  
308 epibionts of *Trichodesmium* [44] and were likely attached to the colonies as they sunk  
309 from the surface ocean into the traps. The other most prevalent group was  
310 Deltaproteobacteria, with genera such as *Desulfatibacillum*, *Desulfobacter*,  
311 *Desulfolobus*, and *Desulfovibrio* together comprising 12.5% of cDNA reads on average.  
312 This group has not been previously identified as an epibiont of *Trichodesmium* but is  
313 commonly observed in sinking particles intercepted with sediment traps in the dark  
314 ocean [21].

315

### 316 *Sinking Trichodesmium simulation experiments*

317

318 We confirmed the ability of *Trichodesmium* to fix N<sub>2</sub> under mesopelagic conditions using  
319 a particle sinking simulator (see Methods; [42]). *Trichodesmium* cultures submitted to

320 increasing hydrostatic pressure for 192 and 360 h in the dark (equivalent to 150 and 300  
321 m simulated depth) had  $^{15}\text{N}$  atom % enrichment values of  $0.375 \pm 0.012$  and  $0.370 \pm$   
322  $0.002$  atom %, respectively (Fig. 3A), indicating low but measurable  $\text{N}_2$  fixation. Control  
323 *Trichodesmium* cultures kept at ambient lab pressure conditions had  $^{15}\text{N}$  atom %  
324 enrichments of  $0.390 \pm 0.012$  and  $0.393 \pm 0.008$  after 192 and 360 h of incubation,  
325 respectively (Fig. 3B). This difference in pressurized (Fig. 3A) and non-pressurized (Fig.  
326 3B)  $\text{N}_2$  fixation rates is in agreement with previous metabolic rate slowdown in epipelagic  
327 prokaryotes submitted to mesopelagic pressure levels [45] and indicates that increasing  
328 pressure reduces but does not completely incapacitate  $\text{N}_2$  fixation in *Trichodesmium*. We  
329 however note that while the sinking simulator allows changing pressure and  
330 temperature along the simulated sinking process, it does not allow changing nutrient  
331 concentrations. The increasing concentrations of nitrate with depth in the mesopelagic  
332 may inhibit  $\text{N}_2$  fixation. Thus, the rates measured in these sinking simulations represent  
333 a non-inhibited upper limit of diazotrophic activity.

334

335 *How does Trichodesmium obtain energy to fix  $\text{N}_2$  at depth?*

336

337 *Trichodesmium* uses photosynthetically fixed carbon to fuel the energetically expensive  
338 process of  $\text{N}_2$  fixation [46]. Hence, the dark conditions of the mesopelagic ocean should  
339 be expected to halt photosynthesis and  $\text{N}_2$  fixation in *Trichodesmium*, eventually leading  
340 to its death. We hypothesized that *Trichodesmium* can fix  $\text{N}_2$  in the dark ocean using  
341 stored intracellular carbon acquired by photosynthesis before starting to sink. To test  
342 how much carbon storage *Trichodesmium* would need to fix  $\text{N}_2$  until reaching 1 000 m of  
343 depth (corresponding to our field observations), we adapted a published cell metabolism  
344 model [47] (Fig. S2). The model simulates changes in intracellular carbon storage (the

345 ratio of carbon storage to biomass or  $R_{Sto}$ ) while sinking linearly in the water column over  
346 a wide range of sinking velocities. The model output provides a relationship between the  
347 cell's initial  $R_{Sto}$  ( $R_{Sto}$  value before starting to sink) and the depth at which carbon storage  
348 depletes (Fig. 4).

349

350 Considering that *Trichodesmium* starts sinking below the mixed layer depth (~40 m; Fig.  
351 S2), the cell's metabolism becomes dependent on intracellular carbon storage when light  
352 is extinguished (~170 m; Fig. S2). Below that depth,  $R_{Sto}$  decreases (Fig. 4). When the  
353 initial  $R_{Sto} = 1$  (which is at the lower end of the range measured in phytoplankton, see  
354 Methods), the cell's carbon storage is depleted at around 750 m assuming a medium  
355 sinking velocity of 375 m d<sup>-1</sup> (yellow dot in Fig. 4). With a higher initial  $R_{Sto}$  of 1.3 and the  
356 same sinking velocity, carbon storage is depleted at 1 000 m. This suggests that an  
357 initial  $R_{Sto}$  of at least 1.3 is required for *Trichodesmium* cells to reach 1 000 m of depth  
358 with enough carbon to sustain N<sub>2</sub> fixation (pink dot in Fig. 4) and be consistent with our  
359 field data (Fig. 1). We also note that *Trichodesmium* may obtain carbon from dissolved  
360 organic matter available in their surrounding medium [40], which is not modeled here.  
361 This could decrease the required initial  $R_{Sto}$  to sustain N<sub>2</sub> fixation at 1000 m depth.

362

363 *Trichodesmium* invests a significant part of its carbon storage in maintaining low  
364 intracellular oxygen concentrations through respiratory protection [47, 48]. The decrease  
365 in temperature with depth slows down *Trichodesmium*'s metabolism, decreasing the  
366 speed of oxygen diffusion (Walden's rule [47]), which reduces the level of respiratory  
367 protection needed to fix N<sub>2</sub> and decreasing and thus carbon storage consumption. While  
368 the decrease in temperature with depth also increases the saturated concentration of  
369 oxygen, the concentration of oxygen below the mixed layer in our field experiment was

370 under-saturated (Fig. S2), with oxygen deficit particularly pronounced below 600 m. The  
371 combined effects of declining temperatures and oxygen under-saturation contribute to  
372 the reduction in carbon storage consumption and are reflected as an increasing slope in  
373 the non-linear curve in Fig. 4.

374

375 The high nitrate concentrations of the mesopelagic ocean could inhibit  $N_2$  fixation in  
376 *Trichodesmium* [49]. While no studies have explicitly tested the inhibition of  $N_2$  fixation  
377 by nitrate in the mesopelagic, we explored this effect by considering two constant levels  
378 of inhibition (70% and 50%; Fig. S3), which are in the upper range of previous culture  
379 and field studies [50]. The model predicts that under 70% and 50% inhibition the  
380 required initial  $R_{Sto}$  decreases to  $\sim 0.5$  and  $\sim 0.8$ , respectively (Fig. S3). This indicates that  
381 when nitrate inhibits  $N_2$  fixation less carbon storage is consumed, allowing  
382 *Trichodesmium* to remain metabolically active at deeper depths (Fig. S3). Previous  
383 studies have shown that *Trichodesmium* can fix  $N_2$  in the presence of up to 20  $\mu M$  nitrate  
384 provided phosphate concentrations are high enough to sustain growth [50]. At the  
385 depths where traps were deployed during our field experiment, excess phosphate with  
386 respect to nitrate according to the Redfield stoichiometry of 16:1 ( $P^*$  parameter; Fig. S2)  
387 likely permitted  $N_2$  fixation (Fig. 1). Finally, the increased partial pressure of  $CO_2$  with  
388 depth could also favor  $N_2$  fixation in *Trichodesmium* as previously shown in culture  
389 experiments [51].

390

391 *Is fast sinking necessary for Trichodesmium to fix  $N_2$  in the mesopelagic?*

392

393 Previous studies have suggested that viable and/or active growing cyanobacteria in the  
394 dark ocean are associated with fast-sinking particles, mineral ballasting, or episodic flux

395 events [17, 18, 52]. While the gas vesicles of *Trichodesmium* may prevent it from  
396 sinking, a previous study found that sinking *Trichodesmium* can contribute importantly to  
397 organic matter export during atmospheric dust ballasting events [50]. Three months  
398 before our cruise, a volcano erupted over the Tonga-Kermadec volcanic arc [53]. This  
399 volcano was particularly close to station S10M (~144 km). Measurements of lithogenic  
400 silica in the trap material (Supplementary Methods) showed that the lithogenic to  
401 particulate organic matter ratio of particulate matter was maximal at station S10M (Table  
402 S4). Scanning electron microscopy images (Supplementary Methods) showed volcanic  
403 materials intermingled with *Trichodesmium* filaments (Fig. S4), particularly at the 1 000  
404 m trap of station S10M where *Trichodesmium nifH* gene transcripts were more abundant  
405 (Fig. 2). Hence, the eruption may have stimulated fast sinking by *Trichodesmium*,  
406 particularly at the S10M site. However, both our laboratory sinking simulations and the  
407 results of the cell metabolic model indicate that *Trichodesmium* can fix N<sub>2</sub> within the  
408 mesopelagic depth range even when sinking at low velocity (e.g. 20 m d<sup>-1</sup>).

409

#### 410 Potential impact of sinking *Trichodesmium* on mesopelagic prokaryotic communities

411

412 *Trichodesmium* releases up to 19% of the N<sub>2</sub> fixed as ammonium [54], which is the main  
413 energy source for dark CO<sub>2</sub> fixation by the abundant Thaumarchaeota [55]. Considering  
414 the *Trichodesmium*-specific N<sub>2</sub> fixation rates measured here and a ratio of dark CO<sub>2</sub>  
415 fixed per ammonium oxidized of 0.1 [56, 57], the ammonium released by sinking  
416 *Trichodesmium* may sustain CO<sub>2</sub> fixation rates of up to 0.2 μmol C m<sup>-3</sup> d<sup>-1</sup>. This  
417 represents ~13% of previous dark CO<sub>2</sub> fixation rates measured in the mesopelagic  
418 ocean [58]. However, to date very few dark CO<sub>2</sub> fixation measurements are available

419 and their magnitude in *Trichodesmium*-dominated regions (particularly in the South  
420 Pacific Ocean) is unknown.

421

422 More importantly, *Trichodesmium* releases ca. 50% of its fixed N<sub>2</sub> as dissolved organic  
423 nitrogen [59], which mostly composed of labile amino acids [60]. The mycosporine and  
424 tryptophan-like compound optical signatures observed at >1 000 m in our study are  
425 consistent with previous measurements of natural [61–63] and cultured *Trichodesmium*  
426 colonies (Supplementary Methods; Fig. S6). These signals were particularly strong at  
427 S10M (Fig. S5) coinciding with highest *Trichodesmium nifH* transcripts (Fig. 2) and  
428 supporting the active release of amino acids by sinking *Trichodesmium*. Amino acids  
429 released by active sinking *Trichodesmium* could add up to the labile compounds  
430 released by sinking particles in the dark ocean [64–67], contributing to the prokaryotic  
431 respiration organic matter [68] in the subtropical and tropical regions where  
432 *Trichodesmium* occurs.

433

## 434 **Conclusions**

435

436 This study provides the first cell-specific N<sub>2</sub> fixation rates, nitrogenase expression and  
437 metabolic mechanistic understanding of *Trichodesmium* sinking into the mesopelagic  
438 zone, representing a step forward from early findings of viable surface ocean  
439 phytoplankton at depth. Diazotrophically active *Trichodesmium* can provide mesopelagic  
440 bacteria and archaea with ammonium and labile amino acids, contributing to  
441 chemolithoautotrophy and organic matter remineralization in the mesopelagic zone,  
442 respectively. The balance between these two processes sets the ultimate role of the  
443 dark ocean in carbon sequestration with consequences for global climate. Given the

444 widespread blooms of *Trichodesmium* in the surface ocean, which are predicted to  
445 expand due to climate change [42], we contend that the impact of sinking  
446 *Trichodesmium* on the biogeochemistry of the dark ocean needs to be considered in  
447 carbon sequestration models.

448

#### 449 **Acknowledgments**

450

451 The authors would like to thank the crew and technical staff of R/V *L'Atalante* as well as  
452 the scientists that participated in trap deployment onboard, as well as N. Brouilly and F.  
453 Richard at the IBDML SEM facility (Marseille, France). We are indebted to A. Vogts for  
454 nanoSIMS analyses (IOW, Warnemünde, Germany) and A. Filella (MIO, Marseille,  
455 France) for salinity effect experiments on *Trichodesmium* cultures. This research was  
456 supported by Agence Nationale de Recherche grant ANR-18-CE01-0016 (SB), A\*Midex  
457 grant TONGA (SB), Institut National des Sciences de l'Univers Les Enveloppes Fluides  
458 et l'Environnement (INSU-LEFE) grant TONGA (SB), INSU-LEFE grant DEFINE (MB),  
459 National Science Foundation EPSCoR Cooperative Agreement OIA-1655221 E (KI) and  
460 Danish Council for independent research 6108-00013 (SH and LR). The authors are  
461 grateful to M. Sebastián, J.M. Gasol, J. Arístegui and X.A. Álvarez-Salgado for their  
462 comments on previous versions of this manuscript.

463

464 **Competing Interests:** Authors declare that they have no competing interests.

465

466 **Data Availability Statement:** All data are available in the main text or the  
467 supplementary materials. The model code for this study can be found in

468 <https://zenodo.org/record/5153594> (DOI: 10.5281/zenodo.5153594). Sequences have  
469 been deposited in the Sequence Read Archive under accession number PRJNA742179.

470 **References**

471

- 472 1. Gruber N, Galloway JN. An Earth-system perspective of the global nitrogen cycle.  
473 *Nature* 2008; **451**: 293–296.
- 474 2. Hutchins DA, Capone DG. The marine nitrogen cycle: new developments and global  
475 change. *Nat Rev Microbiol* 2022.
- 476 3. Zehr JP, Capone DG. Changing perspectives in marine nitrogen fixation. *Science*  
477 2020; **368**: eaay9514.
- 478 4. Bombar D, Paerl RW, Riemann L. Marine Non-Cyanobacterial Diazotrophs: Moving  
479 beyond Molecular Detection. *Trends Microbiol* 2016; **24**: 916–927.
- 480 5. Benavides M, Moisander PH, Berthelot H, Dittmar T, Grosso O, Bonnet S.  
481 Mesopelagic N<sub>2</sub> fixation related to organic matter composition in the Solomon and  
482 Bismarck Seas (Southwest Pacific). *PLoS One* 2015; **10**: 1–19.
- 483 6. Rahav E, Bar-Zeev E, Ohayon S, Elifantz H, Belkin N, Herut B, et al. Dinitrogen  
484 fixation in aphotic oxygenated marine environments. *Front Microbiol* 2013; **4**: 1–11.
- 485 7. Benavides M, Bonnet S, Berman-frank I, Riemann L. Deep Into Oceanic N<sub>2</sub>  
486 Fixation. *Frontiers Marine Science* 2018; **5**: 108.
- 487 8. Capone DG, Burns JA, Montoya JP, Subramaniam A, Mahaffey C, Gunderson T, et  
488 al. Nitrogen fixation by *Trichodesmium* spp.: An important source of new nitrogen to  
489 the tropical and subtropical North Atlantic Ocean. *Global Biogeochem Cycles* 2005;  
490 **19**: 1–17.
- 491 9. Villareal TA, Carpenter EJ. Diel buoyancy regulation in the marine diazotrophic  
492 cyanobacteria *Trichodesmium thiebautii*. *Limnol Oceanogr* 1990; **35**: 1832–1837.
- 493 10. White AE, Spitz YH, Letelier RM. Modeling carbohydrate ballasting by  
494 *Trichodesmium* spp. *Mar Ecol Prog Ser* 2006.

- 495 11. Scharek R, Tupas LM, Karl DM. Diatom fluxes to the deep sea in the oligotrophic  
496 North Pacific gyre at Station ALOHA. *Mar Ecol Prog Ser* 1999; **182**: 55–67.
- 497 12. Guidi L, Calil PHR, Duhamel S, Björkman KM, Doney SC, Jackson GA, et al. Does  
498 eddy-eddy interaction control surface phytoplankton distribution and carbon export  
499 in the North Pacific Subtropical Gyre? *Journal of Geophysical Research:*  
500 *Biogeosciences* 2012.
- 501 13. Pabortsava K, Lampitt RS, Benson J, Crowe C, McLachlan R, Le Moigne FAC, et  
502 al. Carbon sequestration in the deep Atlantic enhanced by Saharan dust. *Nat*  
503 *Geosci* 2017; **10**: 189–194.
- 504 14. Bar-Zeev E, Avishay I, Bidle KD, Berman-Frank I. Programmed cell death in the  
505 marine cyanobacterium *Trichodesmium* mediates carbon and nitrogen export. *ISME*  
506 *J* 2013.
- 507 15. Smayda TJ. Normal and accelerated sinking of phytoplankton in the sea. *Mar Geol*  
508 1971; **11**: 105–122.
- 509 16. Agustí S, González-Gordillo JI, Vaqué D, Estrada M, Cerezo MI, Salazar G, et al.  
510 Ubiquitous healthy diatoms in the deep sea confirm deep carbon injection by the  
511 biological pump. *Nat Commun* 2015; **6**: 1–8.
- 512 17. Sohrin R, Isaji M, Obara Y, Agostini S, Suzuki Y, Hiroe Y, et al. Distribution of  
513 *Synechococcus* in the dark ocean. *Aquat Microb Ecol* 2011; **64**: 1–14.
- 514 18. Lochte K, Turley CM. Bacteria and cyanobacteria associated with phytodetritus in  
515 the deep sea. *Nature* 1988; **333**: 67–69.
- 516 19. Smith DC, Simon M, Alldredge AL, Azam F. Intense hydrolytic enzyme activity on  
517 marine aggregates and implications for rapid particle dissolution. *Nature* 1992; **359**:  
518 139–142.

- 519 20. Kana TM, Darkangelo C, Hunt MD, Oldham JB, Bennett GE, Cornwell JC.  
520 Membrane Inlet Mass Spectrometer for Rapid Environmental Water Samples. *Anal*  
521 *Chem* 1994; **66**: 4166–4170.
- 522 21. Fontanez KM, Eppley JM, Samo TJ, Karl DM, DeLong EF. Microbial community  
523 structure and function on sinking particles in the North Pacific Subtropical Gyre.  
524 *Front Microbiol* 2015; **6**.
- 525 22. Boyd PW, McDonnell A, Valdez J, LeFevre D, Gall MP. RESPIRE: An in situ particle  
526 interceptor to conduct particle remineralization and microbial dynamics studies in  
527 the oceans' Twilight Zone. *Limnol Oceanogr Methods* 2015; **13**: 494–508.
- 528 23. Caffin M, Moutin T, Ann Foster R, Bouruet-Aubertot P, Michelangelo Doglioli A,  
529 Berthelot H, et al. N<sub>2</sub> fixation as a dominant new N source in the western tropical  
530 South Pacific Ocean (OUTPACE cruise). *Biogeosciences* 2018.
- 531 24. Polerecky L, Adam B, Milucka J, Musat N, Vagner T, Kuypers MMM.  
532 Look@NanoSIMS - a tool for the analysis of nanoSIMS data in environmental  
533 microbiology. *Environ Microbiol* 2012; **14**: 1009–1023.
- 534 25. Montoya JP, Voss M, Kahler P, Capone DG. A Simple, High-Precision, High-  
535 Sensitivity Tracer Assay for N<sub>2</sub> Fixation. *Appl Environ Microbiol* 1996; **62**: 986–993.
- 536 26. Bonnet S, Benavides M, Camps M, Torremocha A, Grosso O, Spungin D, et al.  
537 Massive export of diazotrophs across the tropical south Pacific Ocean. *bioRxiv* .  
538 2021. , 2021.05.07.442706
- 539 27. Meiler S, Britten GL, Dutkiewicz S, Gradoville MR, Moisander PH, Jahn O, et al.  
540 Constraining uncertainties of diazotroph biogeography from nifH gene abundance.  
541 *Limnol Oceanogr* 2022.
- 542 28. Redfield AC. The influence of organisms on the composition of seawater. *The sea*  
543 1963; **2**: 26–77.

- 544 29. Zehr JP, Mellon MT, Zani S. New nitrogen-fixing microorganisms detected in  
545 oligotrophic oceans by amplification of nitrogenase (nifH) genes. *Appl Environ*  
546 *Microbiol* 1998; **64**: 3444–3450.
- 547 30. Callahan BJ, McMurdie PJ, Rosen MJ, Han AW, Johnson AJA, Holmes SP.  
548 DADA2: High-resolution sample inference from Illumina amplicon data. *Nat Methods*  
549 2016; **13**: 581–583.
- 550 31. Wang Q, Quensen JFI, Fish JA, Lee TK, Sun Y, Tiedje JM, et al. Ecological patterns  
551 of nifH genes in four terrestrial climatic zones Explored with Targeted  
552 Metagenomics Using FrameBot, a New Informatics Tool. *MBio* 2013; **4**: 1–9.
- 553 32. Angel R, Nepel M, Panhölzl C, Schmidt H, Herbold CW, Eichorst SA, et al.  
554 Evaluation of primers targeting the diazotroph functional gene and development of  
555 NifMAP - A bioinformatics pipeline for analyzing nifH amplicon data. *Front Microbiol*  
556 2018.
- 557 33. Tamburini C, Goutx M, Guigue C, Garel M, Lefèvre D, Charrière B, et al. Effects of  
558 hydrostatic pressure on microbial alteration of sinking fecal pellets. *Deep Sea Res*  
559 *Part 2 Top Stud Oceanogr* 2009; **56**: 1533–1546.
- 560 34. Chen Y-B, Zehr JP, Mellon M. Growth and nitrogen fixation of the diazotrophic  
561 filamentous nonheterocystous cyanobacterium *Trichodesmium* sp. IMS 101 in  
562 defined media: evidence for a circadian rhythm. *J Phycol* 1996; **32**: 916–923.
- 563 35. Inomura K, Deutsch C, Wilson ST, Masuda T, Lawrenz E, Sobotka R, et al.  
564 Quantifying Oxygen Management and Temperature and Light Dependencies of  
565 Nitrogen Fixation by *Crocospaera watsonii*. *MSphere* 2019; **4**: 1–15.
- 566 36. Fernandez AC, Phillis GDJ. Temperature dependence of the diffusion coefficient of  
567 polystyrene latex spheres. *Biopolymers* 1983; **22**: 593–595.

- 568 37. Chakraborty S, Andersen KH, Visser AW, Inomura K, Follows MJ, Riemann L.  
569 Quantifying nitrogen fixation by heterotrophic bacteria in sinking marine particles. 2–  
570 4.
- 571 38. Liefer JD, Garg A, Fyfe MH, Irwin AJ, Benner I, Brown CM, et al. The  
572 Macromolecular Basis of Phytoplankton C:N:P Under Nitrogen Starvation. *Front*  
573 *Microbiol* 2019; **10**: 763.
- 574 39. Berthelot H, Bonnet S, Grosso O, Cornet V, Barani A. Transfer of diazotroph-  
575 derived nitrogen towards non-diazotrophic planktonic communities: A comparative  
576 study between *Trichodesmium erythraeum* *Crocospaera watsonii* and *Cyanothece*  
577 *sp.* *Biogeosciences* 2016; **13**: 4005–4021.
- 578 40. Benavides M, Berthelot H, Duhamel S, Raimbault P, Bonnet S. Dissolved organic  
579 matter uptake by *Trichodesmium* in the Southwest Pacific. *Sci Rep* 2017; **7**: 1–6.
- 580 41. Pade N, Michalik D, Ruth W, Belkin N, Hess WR, Berman-Frank I, et al.  
581 Trimethylated homoserine functions as the major compatible solute in the globally  
582 significant oceanic cyanobacterium *Trichodesmium*. *Proc Natl Acad Sci U S A* 2016;  
583 **113**: 13191–13196.
- 584 42. Boatman TG, Upton GJG, Lawson T, Geider RJ. Projected expansion of  
585 *Trichodesmium*'s geographical distribution and increase in growth potential in  
586 response to climate change. *Glob Chang Biol* 2020; **26**: 6445–6456.
- 587 43. Dai X, Wang B-J, Yang Q-X, Jiao N-Z, Liu S-J. *Yangia pacifica* gen. nov., sp. nov., a  
588 novel member of the *Roseobacter* clade from coastal sediment of the East China  
589 Sea. *Int J Syst Evol Microbiol* 2006; **56**: 529–533.
- 590 44. Frischkorn KR, Rouco M, Van Mooy BAS, Dyhrman ST. Epibionts dominate  
591 metabolic functional potential of *Trichodesmium* colonies from the oligotrophic  
592 ocean. *ISME J* 2017.

- 593 45. Tamburini C, Boutrif M, Garel M, Colwell RR, Deming JW. Prokaryotic responses to  
594 hydrostatic pressure in the ocean - a review. *Environ Microbiol* 2013; **15**: 1262–  
595 1274.
- 596 46. Berman-Frank I, Lundgren P, Chen YB, Küpper H, Kolber Z, Bergman B, et al.  
597 Segregation of nitrogen fixation and oxygenic photosynthesis in the marine  
598 cyanobacterium *Trichodesmium*. *Science* 2001; **294**: 1534–1537.
- 599 47. Inomura K, Wilson ST, Deutsch C. Mechanistic Model for the Coexistence of  
600 Nitrogen Fixation and Photosynthesis in Marine *Trichodesmium*. *mSystems* 2019; **4**.
- 601 48. Berman-Frank I, Lundgren P, Falkowski P. Nitrogen fixation and photosynthetic  
602 oxygen evolution in cyanobacteria. *Res Microbiol* 2003; **154**: 157–164.
- 603 49. Holl CM, Montoya JP. Interactions between nitrate uptake and nitrogen fixation in  
604 continuous cultures of the marine diazotroph *Trichodesmium* (Cyanobacteria). *J*  
605 *Phycol* 2005; **41**: 1178–1183.
- 606 50. Knapp AN. The sensitivity of marine N<sub>2</sub> fixation to dissolved inorganic nitrogen.  
607 *Front Microbiol* 2012; **3**.
- 608 51. Hutchins DA, Fu F-X, Zhang Y, Warner ME, Feng Y, Portune K, et al. CO<sub>2</sub> control of  
609 *Trichodesmium* N<sub>2</sub> fixation, photosynthesis, growth rates, and elemental ratios:  
610 Implications for past, present, and future ocean biogeochemistry. *Limnol Oceanogr*  
611 2007; **52**: 1293–1304.
- 612 52. Karl DM, Church MJ, Dore JE, Letelier RM, Mahaffey C. Predictable and efficient  
613 carbon sequestration in the North Pacific Ocean supported by symbiotic nitrogen  
614 fixation. *Proceedings of the National Academy of Sciences* 2012.
- 615 53. Brandl PA, Schmid F, Augustin N, Grevemeyer I, Arculus RJ, Devey CW, et al. The  
616 6–8 Aug 2019 eruption of ‘Volcano F’ in the Tofua Arc, Tonga. *J Volcanol Geotherm*  
617 *Res* 2020; **390**: 106695.

- 618 54. Mulholland MR, Bronk DA, Capone DG. Dinitrogen fixation and release of  
619 ammonium and dissolved organic nitrogen by *Trichodesmium* IMS101. *Aquat*  
620 *Microb Ecol* 2004; **37**: 85–94.
- 621 55. Könneke M, Bernhard AE, De La Torre JR, Walker CB, Waterbury JB, Stahl DA.  
622 Isolation of an autotrophic ammonia-oxidizing marine archaeon. *Nature* 2005; **437**:  
623 543–546.
- 624 56. Bayer B, Vojvoda J, Reinthaler T, Reyes C, Pinto M, Herndl GJ. *Nitrosopumilus*  
625 *adriaticus* sp. nov. and *Nitrosopumilus piranensis* sp. nov., two ammonia-oxidizing  
626 archaea from the Adriatic Sea and members of the class Nitrososphaeria. *Int J Syst*  
627 *Evol Microbiol* 2019; **69**: 1892–1902.
- 628 57. Baltar F, Herndl GJ. Ideas and perspectives: Is dark carbon fixation relevant for  
629 oceanic primary production estimates? *Biogeosciences* 2019; **16**: 3793–3799.
- 630 58. Reinthaler T, van Aken HM, Herndl GJ. Major contribution of autotrophy to microbial  
631 carbon cycling in the deep North Atlantic's interior. *Deep Sea Res Part 2 Top Stud*  
632 *Oceanogr* 2010; **57**: 1572–1580.
- 633 59. Glibert PM, Bronk DA. Release of Dissolved Organic Nitrogen by Marine  
634 Diazotrophic Cyanobacteria. *Applied and Environmental Microbiology* 1994; **60**:  
635 3996–4000.
- 636 60. Sipler RE, Bronk DA, Seitzinger SP, Lauck RJ, McGuinness LR, Kirkpatrick GJ, et  
637 al. *Trichodesmium*-derived dissolved organic matter is a source of nitrogen capable  
638 of supporting the growth of toxic red tide *Karenia brevis*. *Mar Ecol Prog Ser* 2013;  
639 **483**: 31–45.
- 640 61. Steinberg DK, Nelson NB, Carlson CA, Prusak AC. Production of chromophoric  
641 dissolved organic matter (CDOM) in the open ocean by zooplankton and the  
642 colonial cyanobacterium *Trichodesmium* spp. *Mar Ecol Prog Ser* 2004; **267**: 45–56.

- 643 62. Subramaniam A, Carpenter EJ, Karentz D, Falkowski PG. Bio-optical properties of  
644 the marine diazotrophic cyanobacteria *Trichodesmium* spp. I. Absorption and  
645 photosynthetic action spectra. *Limnol Oceanogr* 1999; **44**: 608–617.
- 646 63. Dias A, Kurian S, Thayapurath S. Optical characteristics of colored dissolved  
647 organic matter during blooms of *Trichodesmium* in the coastal waters off Goa.  
648 *Environ Monit Assess* 2020; **192**: 526.
- 649 64. Seidel M, Vemulapalli SPB, Mathieu D, Dittmar T. Marine Dissolved Organic Matter  
650 Shares Thousands of Molecular Formulae Yet Differs Structurally across Major  
651 Water Masses. *Environ Sci Technol* 2022.
- 652 65. Ruiz-González C, Mestre M, Estrada M, Sebastián M, Salazar G, Agustí S, et al.  
653 Major imprint of surface plankton on deep ocean prokaryotic structure and activity.  
654 *Mol Ecol* 2020; **29**: 1820–1838.
- 655 66. Turley CM, Mackie PJ. Bacterial and cyanobacterial flux to the deep NE atlantic on  
656 sedimenting particles. *Deep Sea Res Part 1 Oceanogr Res Pap* 1995; **42**: 1453–  
657 1474.
- 658 67. Bergauer K, Fernandez-Guerra A, Garcia JAL, Sprenger RR, Stepanauskas R,  
659 Pachiadaki MG, et al. Organic matter processing by microbial communities  
660 throughout the Atlantic water column as revealed by metaproteomics. *Proc Natl*  
661 *Acad Sci U S A* 2018; **115**: E400–E408.
- 662 68. Herndl GJ, Reinthaler T. Microbial control of the dark end of the biological pump.  
663 *Nat Geosci* 2013; **6**: 718–724.
- 664

665 **Figure legends**

666

667 **Figure 1.** *Trichodesmium*-specific  $^{15}\text{N}$  atom % enrichment. (A, B) Boxplots showing the  
668 range, average and outliers of  $^{15}\text{N}/^{14}\text{N}$  ratios measured in natural (non  $^{15}\text{N}_2$ -labeled) and  
669  $^{15}\text{N}_2$ -labeled samples from 170 m, 270 m and 1 000 m depth at stations S05M and  
670 S10M, respectively. The number of trichomes scanned per depth is shown over each  
671 box (n values). All *Trichodesmium* filaments analyzed were significantly enriched in  $^{15}\text{N}$ .  
672 Examples of nanoSIMS  $^{15}\text{N}/^{14}\text{N}$  ratio images of *Trichodesmium* filaments sampled at  
673 station S05M showing the  $^{15}\text{N}/^{14}\text{N}$  isotopic ratio enrichment of *Trichodesmium* filaments  
674 according to the color bar. Filaments shown in panel (C) are those not incubated with  
675  $^{15}\text{N}_2$  (natural). The filaments shown in panels (D-F) are those incubated with  $^{15}\text{N}_2$  and  
676 collected from sediment traps deployed at 170, 270 and 1 000 m, respectively. The  
677 same pattern is repeated for station S10M in panels (G-J) The scale bar in nanoSIMS  
678  $^{15}\text{N}/^{14}\text{N}$  ratio images is 5  $\mu\text{m}$ .

679

680 **Figure 2.** Diazotroph community expression profiles. Relative abundance of *nifH* cDNA  
681 reads originating from sediment traps at 170 m, 270 m, and 1 000 m at stations S05M  
682 (A) and S10M (B). Relative abundances were calculated based on  $146\,000 \pm 18\,000$   
683 reads per sample.

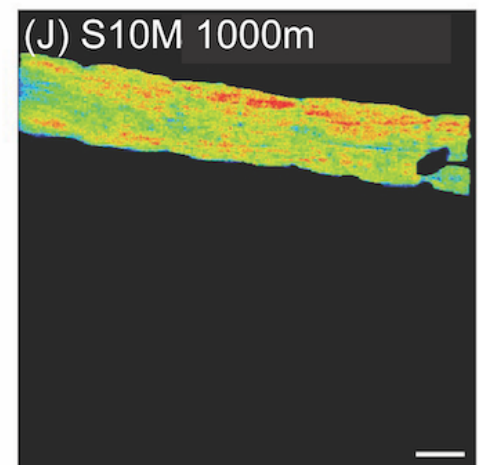
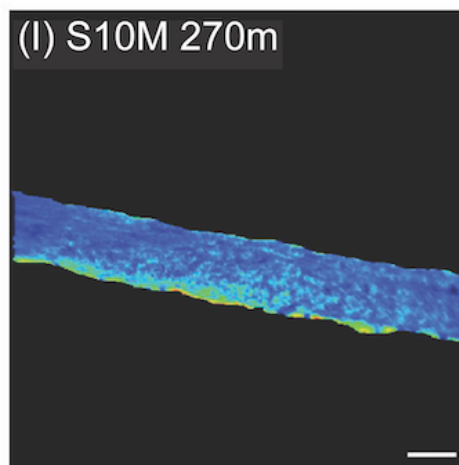
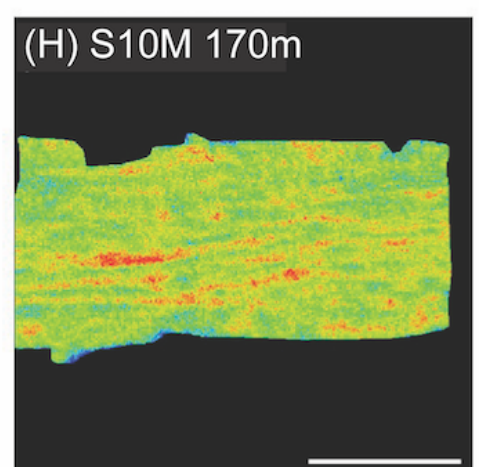
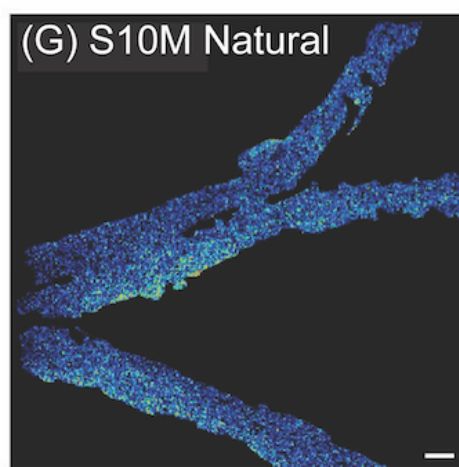
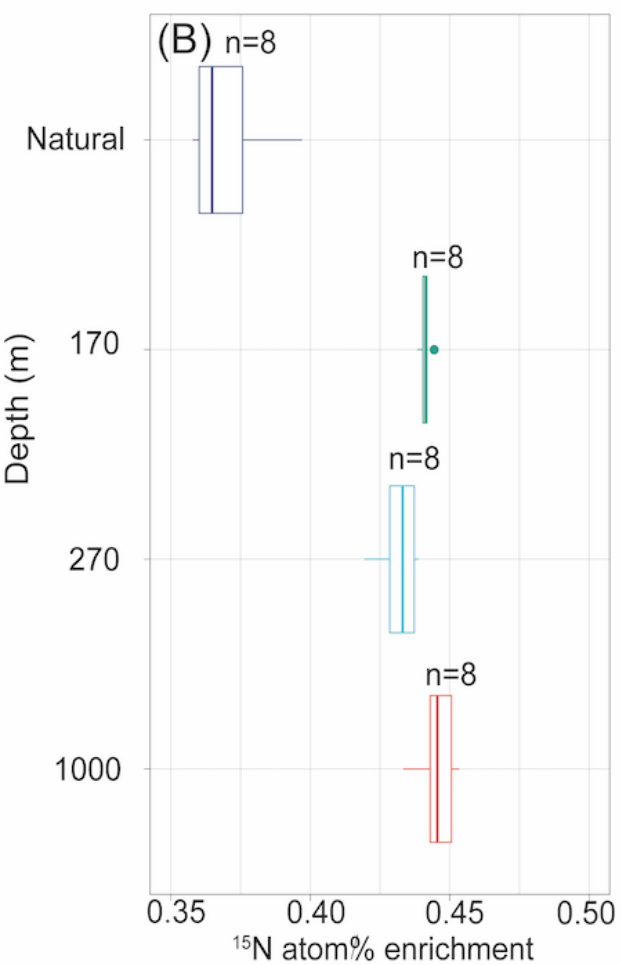
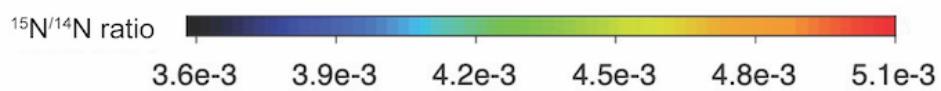
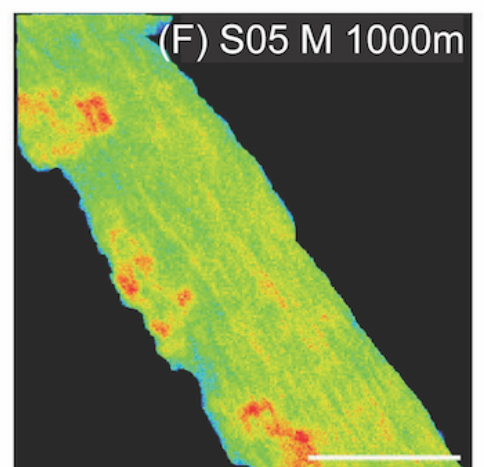
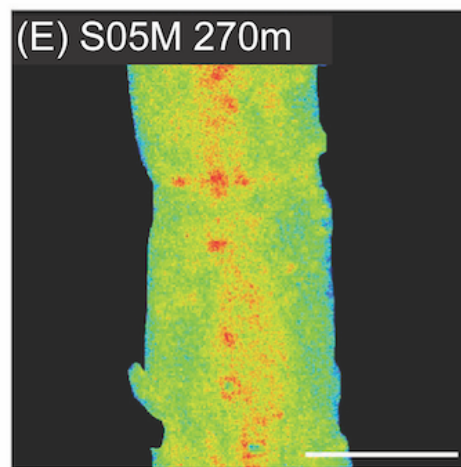
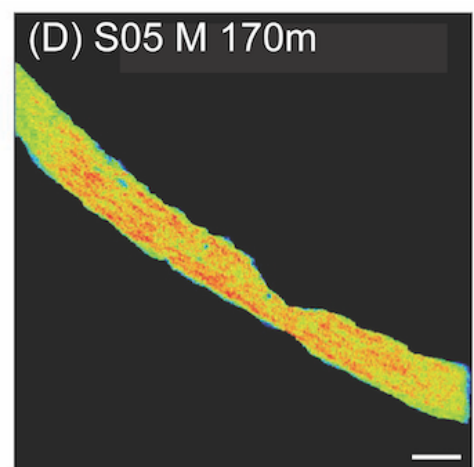
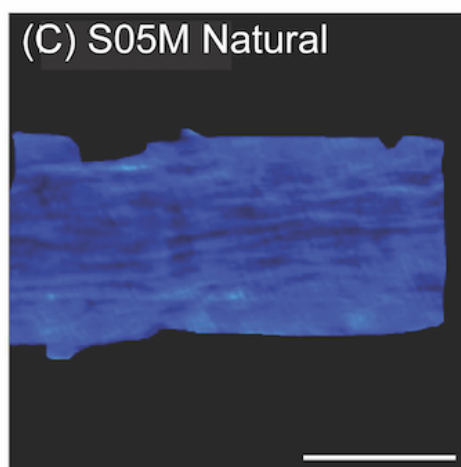
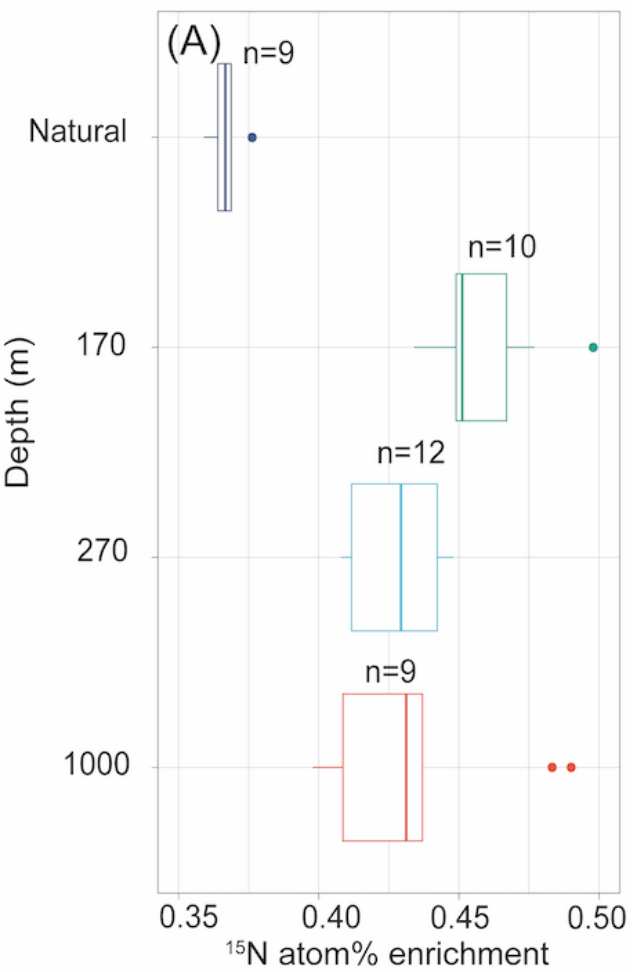
684

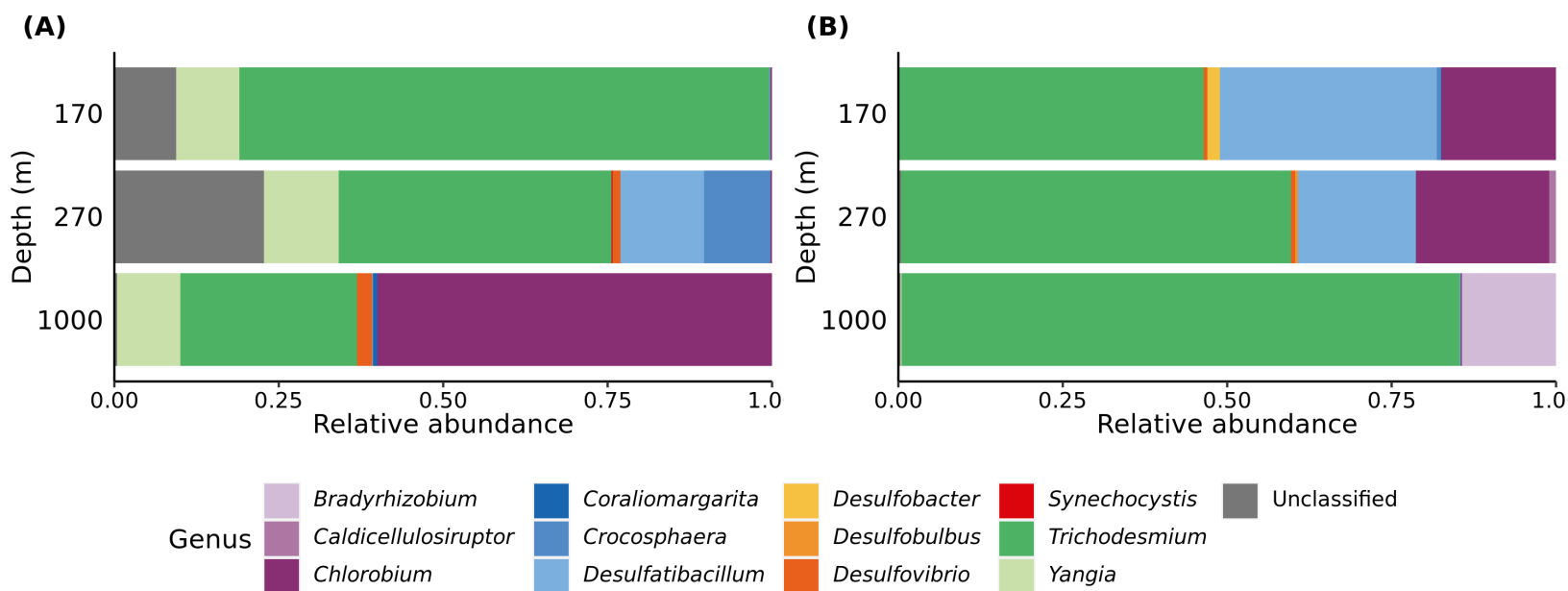
685 **Figure 3.** (A)  $^{15}\text{N}$  atom % enrichment values of triplicate *Trichodesmium* cultures  
686 submitted to a 12h:12h dark:dark light cycle under increasing hydrostatic pressure (0-3  
687 MPa) and decreasing temperature (27 to 14°C) on a sinking particle simulator for 192  
688 and 360 h (simulating 160 and 300 m depth, respectively). (B)  $^{15}\text{N}$  atom % enrichment

689 values of triplicate *Trichodesmium* cultures submitted to a 12h:12h dark:dark at ambient  
690 laboratory pressure and decreasing temperature (27 to 14°C) for 192 and 360 h.

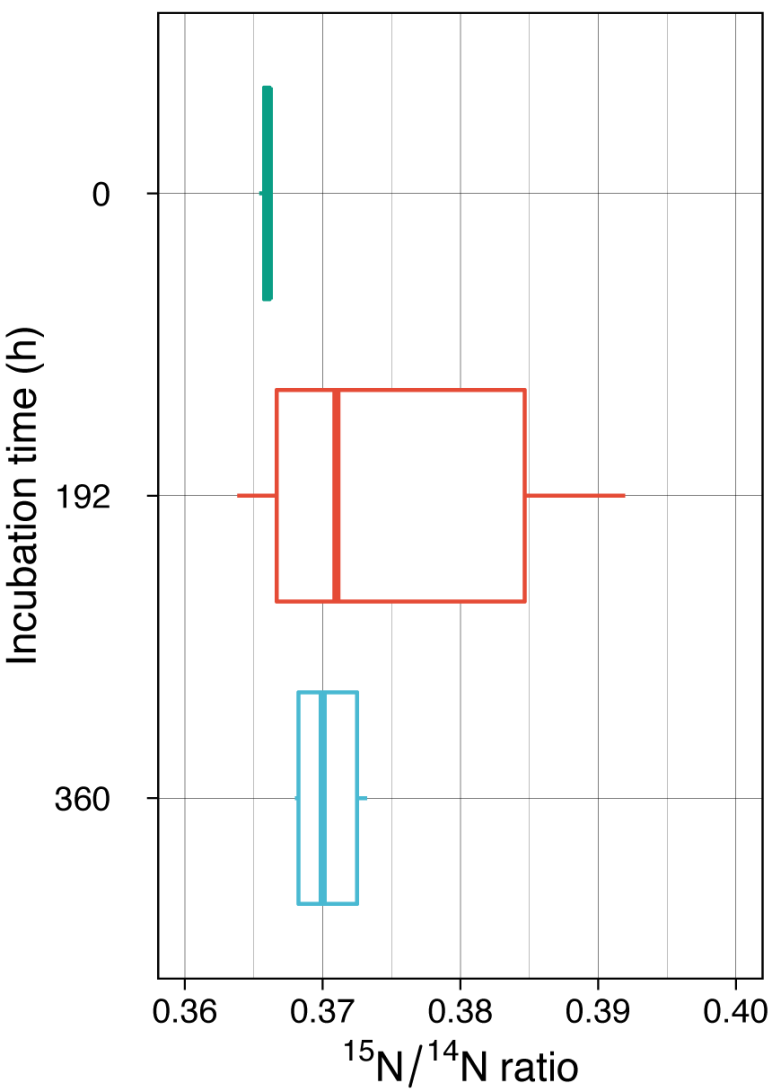
691

692 **Figure 4.** Relationship between the initial carbon storage to biomass ratio (initial  $R_{Sto}$ ) of  
693 *Trichodesmium* cells and the depth at which cell carbon storage is depleted. The x-axis  
694 represents the initial  $R_{Sto}$ , i.e. the carbon storage to biomass ratio of *Trichodesmium* at  
695 40 m (the bottom of the mixing layer, where cells start to sink). The y-axis represents the  
696 depletion depth, i.e. the depth at which carbon storage becomes zero. The blue line  
697 represents the threshold depth below which cell carbon storage is depleted (and thus  $N_2$   
698 fixation is no longer possible) for various initial  $R_{Sto}$  values. The shaded area indicates  
699 the depletion depth range considering the variability in empirical and theoretical sinking  
700 velocities of *Trichodesmium* (Supplementary Methods; Table S2). The yellow and pink  
701 dots indicate the depletion depth for initial  $R_{Sto}$  values of 1 and 1.3, respectively. The  
702 blue line represents the simulation based on the median sinking velocity. The dashed  
703 line indicates the depletion depth of 1 000 m depth. The depletion depth must be below  
704 1 000 m for cells to fix  $N_2$  at 1000 m depth and explain our field observations.





(A) Increasing pressure



(B) Lab ambient pressure

